

Dynamical model for the C_5H_5 cycles in the $C_{60} \cdot 2 Fe(C_5H_5)_2$ solvate

J. Rozen* and F. Masin

Matière Condensée et Résonance Magnétique, Faculté des Sciences, Université Libre de Bruxelles, Boulevard du Triomphe, CP 232, 1050 Brussels, Belgium

R. Céolin

Faculté de Pharmacie, Laboratoire de Chimie Physique, 4 avenue de l'Observatoire, 75270 Paris Cedex 06, France

H. Szwarc

Laboratoire de Chimie Physique, UMR 8000, Université Paris Sud CNRS, bâtiment 490, 91405 Orsay Cedex, France

(Received 27 May 2004; published 29 October 2004)

A model for uniaxial rotation is used in order to calculate the rotational potential for the C_5H_5 rings in the crystal. The contribution from nonbonded interactions is then compared with intra-molecular bounding forces, showing that the observed equilibrium position of the cycles is due to a combination of crystal packing forces and bonding forces within the molecule. The height of the barriers are also extracted and it confirms that there are two kinds of cycles with specific magnetic and electrical environments. The temperature evolution of the spin-lattice relaxation time is probed by 1H NMR spectroscopy over the range 54–394 K and is treated with the model proposed for the simulation. One of the two calculated activation energies is observed in the experimental curve; this indicates coupling with one kind of cycle over the studied temperature range.

DOI: 10.1103/PhysRevB.70.144206

PACS number(s): 71.20.Tx, 76.60.-k, 33.15.Vb, 61.43.Bn

I. INTRODUCTION

Previous x-ray experiments^{1,2} have revealed the structure of the crystal thanks to the apparent immobility of the molecules. The primitive cell is found to be triclinic with space group $P\bar{1}$. As seen in Fig. 1, the crystal is composed by successive superpositions of two layers formed respectively by C_{60} and $Fe(C_5H_5)_2$ (ferrocene) molecules. One of the C_5H_5 cycles (noted Cp for cyclopentadienide) of each ferrocene molecule is situated in a plane parallel to a pentagonal face of the neighboring fullerene, the interplane distance being 3.3 Å. Whereas this value is typical for π interactions between aromatic molecules, the crystal cohesion is found to be due to van der Waals forces. In each ferrocene molecule, the two Cp cycles are nearly parallel since the two Fe-Cp axis form a 178° angle. From the symmetry of the crystal, there are two kinds of inequivalent cycles which are the two Cp cycles of each $Fe(C_5H_5)_2$ molecule. It is shown by DSC² (differential scanning calorimetry) and x-ray measurements that the triclinic structure is conserved between 90 K and 495 K, melting point of the solvate. When lowered from room temperature (RT) to 90 K, temperature does not significantly affect the cell parameters which are modified at a percent order.

Pure ferrocene is known^{3,4} to form a monoclinic phase at RT which transforms into a triclinic phase at 163.9 K. The relative orientations of the Cp cycles in each molecule depend on the phase observed. X-ray diffraction experiments indicate a statistical 2:1 occupancy of the staggered and eclipsed states at RT. Below 163.9 K, it is reported that there is only one equilibrium position for which the deviation angle from the eclipsed configuration is 9° . Moreover, in the $C_{60} \cdot 2$ ferrocene solvate this angle is found to be about 1° . This leads to the conclusion that the packing forces of the

crystals, in which ferrocene takes part, play a non-negligible role in the rotational potential. This has to be computed with the intramolecular contribution which favors eclipsing.^{5,6} Values for the intramolecular reorientation barrier have been deduced from electron diffraction in the gas phase of ferrocene (1.1 kcal/mole from Ref. 5 and 0.9 kcal/mole from Ref. 6).

NMR measurements^{7,8} have been used to characterize the dynamical behavior of the Cp cycles in the $C_{60} \cdot 2$ ferrocene solvate. At RT, two chemical shift tensors for ferrocene have been deduced from a ^{13}C CP-MAS spectrum. This confirms that there are two inequivalent cycles and their symmetry reveals that the cycles are undergoing fast uniaxial rotations compared with the observation time (≈ 0.035 s). Other experiments show that the second order moment of the 1H peak is divided by approximately five upon heating which confirms that uniaxial rotation occurs. As previously

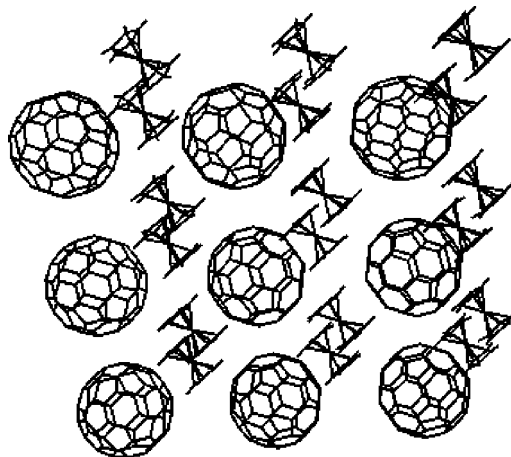


FIG. 1. Packing arrangement of the solvate in the bc plane.

reported,^{2,8,9} this C_{60} solvate is the only one with $C_{60} \cdot 2S_8$ of which a static structure has been fully determined by x-ray diffraction whereas NMR proves the molecules are in fact moving fast enough to average magnetic interactions. This crystallographic motionless appearance can be explained if the molecules undergo quick reorientations between symmetry-equivalent positions. Therefore, the average situation detected by diffraction seems static and dynamics are deduced from NMR experiments which are influenced by the complete motions of atoms.

The present work is divided in two steps. First, the number of activation barriers for Cp cycles and their values are determined from theoretical calculations using interaction potentials. These results lead to conclusions about the role of packing forces, bonded and nonbonded intramolecular contributions. Second, the model defined for calculation is used in order to interpret experimental NMR spin-lattice relaxation measurements.

II. EXPERIMENT

All rotational potential calculations were performed with a C++ program written by the first author.

NMR measurements on protons were done using a Bruker MSL300 spectrometer together with a 7.05 T magnetic field in which 1H spin frequency is 300.13 Mhz. An Oxford ITC4 device was used to regulate the temperature in the HPLP50 probe. Gas flows were needed to avoid gradient between the sample and the thermocouple: air above RT and He/ N_2 at lower temperatures. In order to observe the spin-lattice relaxation time, the saturation-recovery process was used with five $\pi/2$ pulses separated by 500 μs , the length of the $\pi/2$ pulse being adjusted at each temperature.

III. POTENTIAL ENERGY CALCULATIONS

A. Choice of model

The model used to estimate the activation energies for independent rotations of the two types of C_5H_5 rings is based on two assumptions: first, the Cp cycles undergo uniaxial rotations; secondly, there are two inequivalent cycles in each ferrocene molecule.

Attention is focused on one ferrocene molecule, surrounded by an immobile-lattice at the average position. One of the Cp rings was considered to move around its C_5 axis while the other ring, as well as the rest of the lattice remained motionless. This means that no concerted motions were allowed. The justification for such a model comes from the satisfactory agreement with experimental measurements.

Two distinct orientational potentials were deduced by adding by step of 1° the non-bonded interactions of each atom of the cycles with the rest of the lattice. The activation barriers of these potentials plus the bonded contribution can then be compared with experimental results.

B. Potential functions

It has previously been shown that nonbonded activation barriers for reorientational motions can be estimated with a

TABLE I. Values of the parameters of the exponential -6 interaction potential (Ref. 13).

Atom pair	A (kcal/mole \AA^6)	B (kcal/mole)	C (\AA^{-1})
C-C	-535	74461	3.6
H-H	-36	4000	3.74
C-H	-139	9411	3.67

good precision using atom-atom interaction potentials of several kinds.¹⁰⁻¹² The validity of those potentials is restricted by the following assumptions; the interaction energy between two atoms depends only on their nature and on the distance between them. So, the functions do not depend on the molecules involved. As it was done by Campbell *et al.*,¹³ two different potentials were used in the present work.

An exponential -6 function gave the interaction energies between C and H atoms,

$$V = Ar^{-6} + B \exp(-Cr), \quad (1)$$

where V is the energy value and r the distance between the two considered atoms. The potential also depends on three parameters: A , B , and C . Their values, which are given in Table I, have been deduced from experimental results.¹⁴⁻¹⁸

For interactions involving a Fe atom, the Lennard-Jones 6-12 potential was used:

$$V = 4\epsilon [(\sigma/r)^{12} - (\sigma/r)^6]. \quad (2)$$

In this function, the parameter ϵ determines the depth of the potential and σ the distance at which the potential value is zero. Approximate values for these constants have been obtained using the Badger's rule.¹⁹ These are reported in Table II. The reason why such a potential was chosen is only because it does not require experimental results to adjust the parameters; only the row and column of the atom in the Periodic Table are needed. Of course, since it is not based on observations, it is less reliable. But this had a negligible impact on calculations because it was found that the shape of the potential is mainly due to C-C, C-H, and H-H interactions, therefore the Fe atoms influence only the absolute value of the potential but not the height of the energy barriers.

C. Lattice modeling

First, a static lattice was created with data obtained from x-ray experiments at 143 K. This temperature was chosen because it is the lowest temperature at which the positions of each atom of the cell are fully identified. Since no concerted motions are considered, the model is closely related with the

TABLE II. Values of the parameters of the Lennard-Jones 6-12 interaction potential (Ref. 13).

Atom pair	ϵ (kcal/mole)	σ (\AA)
Fe-C	0.262	3.26
Fe-H	0.109	2.34

TABLE III. Values of the lattice vectors and of the cell angles at 143 K (Ref. 1).

<i>a</i>	<i>b</i>	<i>c</i>	α	β	γ
9.899 Å	10.366 Å	11.342 Å	95.55°	90.96°	118.33°

low temperatures situation. The values of the cell constants at 143 K are given in Table III.

In order to manipulate each molecule of a cell more easily, the primitive cell was redefined, so it contains the three entire molecules as shown in Fig. 2. This unit cell is of course still triclinic but does not have a center of inversion. A lattice made of 4³ cells was then created using the vectors *a*, *b*, *c* for translation. The only reason why that number of cells was chosen is because the calculations gave a variation inferior to 10⁻³ kcal/mole for the activation energies if more cells were used. Of course, this is closely related with the shape of the defined potentials and their cutting values.

In the central cell of the lattice, two cycles were considered for rotations. Those were taken in the upper ferrocene molecule represented in Fig. 2. The ring above the Fe atom will be referred as cycle *A* and the other as cycle *B*. Since they had to be entirely modeled for rotation, average values from x-ray measurements were used to rebuild those cycles from the Fe atom previously generated in the static lattice. Two local orthonormal basis were then needed. The *x* axis is defined as the projection of a Fe-C vector, given by x ray, on the plane parallel to the corresponding cycle containing the Fe atom. The *z* axis is the one perpendicular to the ring taking its origin at the position of the Fe atom. In these systems, the average values are given in Table IV. Using this method, the rebuilt cycles have a C₅ symmetry.

D. Results of calculations

As nonbonded interactions could be calculated using the potential functions previously described, it was possible to obtain only the intermolecular contribution by neglecting the effect of the second ring in the ferrocene molecule. This was used as a starting point to study the balance between intra and intermolecular forces. The rotational potential for cycles *A* and *B* are presented on Fig. 3 on which the shift angle 0° corresponds to the one given by x ray, so it represents a deviation of approximately 1° from the eclipsed state.

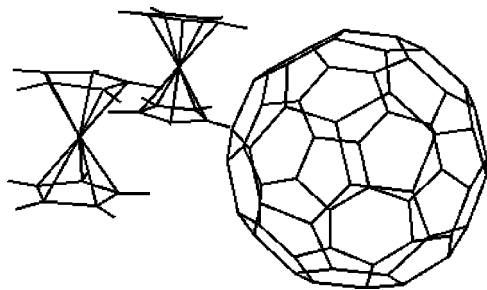


FIG. 2. Primitive cell of the solvate as defined for the simulation.

TABLE IV. Values of the average distances calculated for modeling the moving rings.

Cycle	(Fe-C) _{<i>x</i>}	(Fe-C) _{<i>z</i>}	(Fe-H) _{<i>x</i>}	(Fe-H) _{<i>z</i>}
<i>A</i>	1.217 Å	1.649 Å	2.14 Å	1.666 Å
<i>B</i>	1.214 Å	1.645 Å	2.21 Å	1.532 Å

Obviously, there is only one activation barrier for each cycle and it can be deduced that the two cycles lie in electrically inequivalent sites since the height of the intermolecular barriers are very different. This is an additional information confirming that the cycles are crystallographically and magnetically distinct. Also, it can be seen that the minima are separated multiples of 72° which was expected for a C₅ symmetry. But the more interesting was to find the phasing of the two functions. Both of them have their first minimum at 0° angle which means that the equilibrium positions for the cycles found by x ray are in accordance with those of the packing forces in the crystal.

In order to have a complete description of the reorientational barriers, the previous results were added to the intramolecular contribution deduced from electron diffraction in the gas phase. It was taken from Ref. 6 with parameters

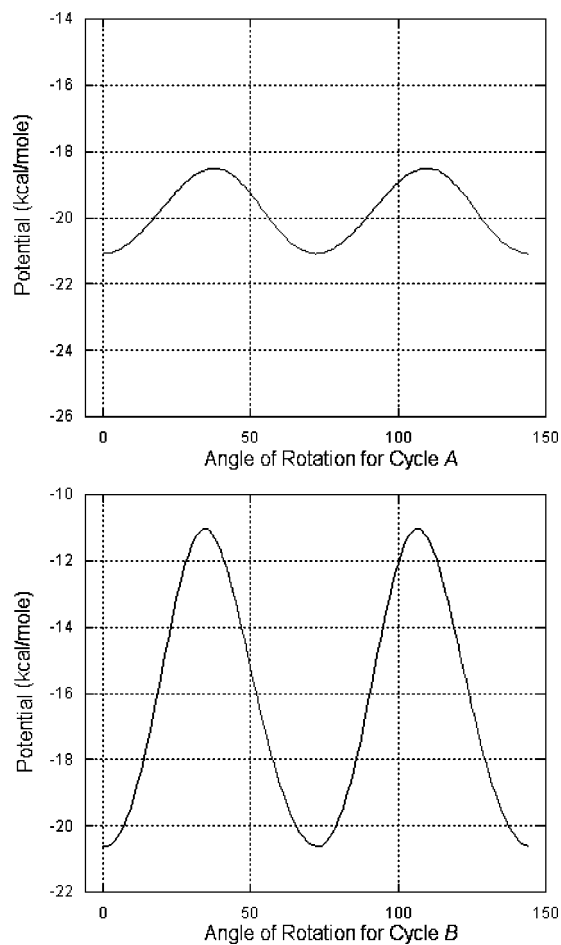


FIG. 3. Intermolecular rotational potential for the two cycles (drawn at the same scale).

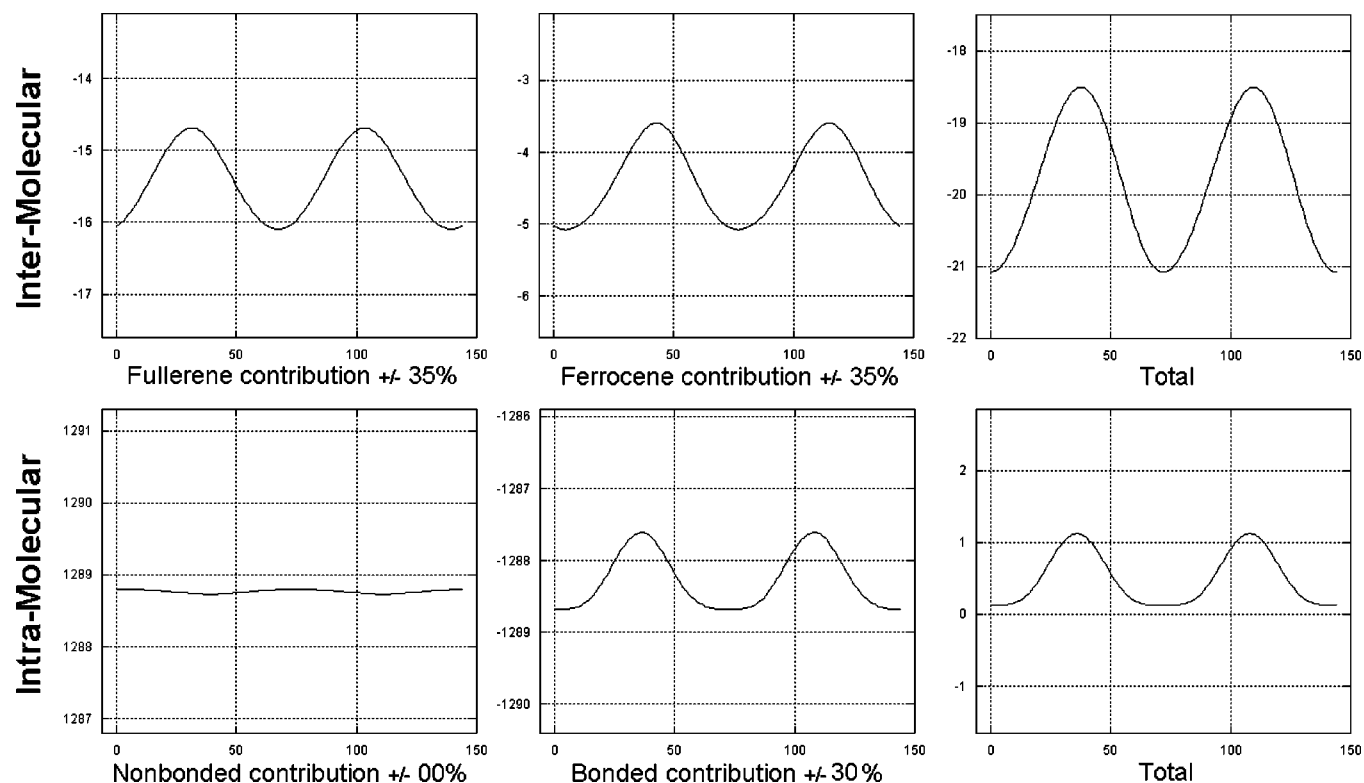


FIG. 4. Different contributions to the rotational potential of cycle A; energies (in kcal/mole) are plotted as a function of angle.

$\beta = -0.25$ and $V_0 = 1$. In the total orientational potentials, the positions of the minima remained the same and the activation barriers have been extracted. The activation energy for rotation is found to be 4.5 kcal/mole for cycle A and 10.5 kcal/mole for cycle B. These values are very different, the one for cycle A being close to what is expected in such a system.

Obviously, the packing forces are the main contribution to the activation energies in the two cases. The nonbonded interaction between the two rings of a molecule was also calculated. Its contribution to the total potential is very small since its height is of the order of 0.1 kcal/mole. However, the repulsion between the atoms of the rings seems to favor a staggered situation but the bonded contribution, which is about ten times greater, has to be the one leading to the eclipsed state observed in the gas phase. These calculations show that the observed crystal structure for ferrocene depends on the balance between packing forces and bonding forces in the molecule. This conclusion, as the one of Campbell *et al.*, contradicts the assumption made by Churchill and Wormald²⁰ who reported that the nonbonded interaction inside the molecule should play a significant role.

Other contributions to the total potential of cycle A were also calculated, as reported on Fig. 4. The forces due only to the neighboring molecules of C_{60} seem to favor an equilibrium position for the rings that would be described by a negative deviation angle from the eclipsed position. But this is balanced by the forces of the rings of the other ferrocene molecules which push the cycle in the opposite way.

For cycle B the contributions to the total potential from molecules of C_{60} , from molecules of ferrocene, from the nonbonding intramolecular forces and from the bonding in-

tramolecular forces are respectively given by approximately 50%, 40%, 00%, and 10%.

This explains the difference between the two activation energies. Indeed, the increased height of the barrier for cycle B is found to be due to the proximity of the neighboring fullerene and ferrocene molecules.

IV. SPIN-LATTICE RELAXATION TIME MEASUREMENTS

A. Hypothesis

Time relaxation measurements are a good way for extracting values of activated motions since T_1 depends on the coupling between the energy of the spins and the dynamics which occur in a sample. The temperature dependence of the 1H spin lattice relaxation time for a motion that can be described by a single correlation time τ is given by the formula of Bloembergen, Purcell and Pound²¹ which was modified by Kubo and Tomita:²²

$$\frac{1}{T_1} = A \left\{ \frac{\tau}{1 + \omega^2 \tau^2} + \frac{4\tau}{1 + 4\omega^2 \tau^2} \right\}. \quad (3)$$

In Eq. (3), ω is the Larmor frequency of the protons in the magnetic field and A is a constant depending on the distances between 1H atoms which gives the amplitude of the energy field modulated by the motion. For an activated process $\tau(T)$ is described by the Arrhenius law

$$\tau = \tau_0 \exp(E_a/RT), \quad (4)$$

where τ_0 is a constant and E_a is the height of the activation

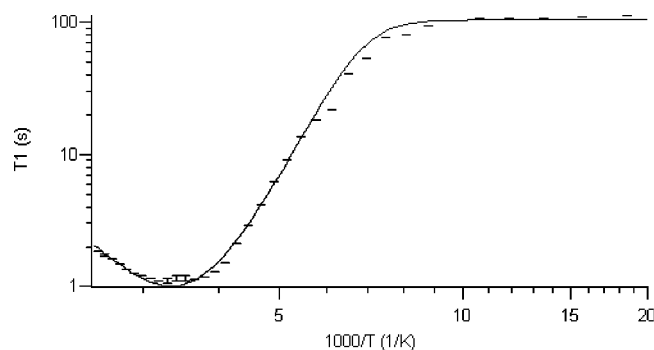


FIG. 5. Spin-lattice relaxation time probed by ¹H NMR spectroscopy over the temperature range 54–394 K. The solid curve is the result of the fit with Eq. (6).

barrier. If the motions in a sample are described by more than one correlation time, the value of T_{total} is given by

$$\frac{1}{T_{\text{total}}} = \sum_i \frac{1}{T_{1i}}, \quad (5)$$

in which each T_{1i} is given by Eq. (3) with the corresponding activation energy and constant A .

In the present work, T_1 was obtained over the temperature range 54–394 K. As shown in Fig. 5, the curve has only one minimum over this range. Also, the recovery curve at each temperature can be described by a single exponential $M_0 [1 - \exp(-t/T_1)]$, M_0 being the equilibrium magnetization. From these observations, it was concluded that the fitting function should contain only one correlation time. Moreover, a constant B was added to Eq. (3) in order to describe the spin-lattice relaxation which is due to other mechanisms, assumed to have a much smaller temperature dependence than the thermally activated jumps on which attention is focused here. Using $1/T_1$ as described in Eq. (3), the fitting function is then given by

$$\frac{1}{T_{1'}} = \frac{1}{T_1} + B. \quad (6)$$

B. Results

The fitting of the experimental data with Eq. (6) is also shown in Fig. 5. It can be seen that the hypothesis of a single activated process seems to modelize the curve well. The values of the parameters appearing in the fitting function are reported in Table V.

TABLE V. Values of the fitting parameters found for the T_1 curve.

E_a	3.4 kcal/mole	\pm	2.5×10^{-3} kcal/mole
τ_0	1.2×10^{-12} s	\pm	6.9×10^{-15} s
A	1.3×10^9 Hz ²	\pm	1.8×10^6 Hz ²
B	9.6×10^{-3} Hz	\pm	1.4×10^{-5} Hz

The energy found is approximately the same as the one calculated for the rotation of cycle A. Moreover, the value of the constant A appearing in Eq. (3) was approximated by calculating a sum on the network for this cycle and it is very close to the fitting value. This suggests that the observed T_1 reduction is only due to the activation of the rotation with the smaller energy barrier. It does not mean that the others cycles are motionless but that the coupling at the studied Larmor frequency over the observed temperature range is effective for cycle A only.

V. CONCLUSIONS

The model used in the simulation is coherent with the observed situation. After M_2 and CSA experiments, it is one more proof that uniaxial rotations occur in the crystal. From calculations, it has been shown that the two kinds of cycles are in different electrical environments. This is seen in the rotational potentials in which two distinct activation barriers were deduced. For the cycle A, a very similar value was observed in the T_1 curve fitted with a single correlation time model.

However, the energy for cycle B was not observed in the curve and is not very likely to be found with this setup since the activation barrier is too high to be observed before melting. In order to detect this specific motion, calculations on the reduction of the M_2 curve are being performed and should lead to the observation of all energies responsible for rotation. Also, as the correlation time of cycle B is believed to be larger, the coupling of its motion with the frequency of the spins would be enhanced at lower fields, allowing the detection of a corresponding minimum value for T_1 .

ACKNOWLEDGMENTS

J.R. and F.M. would like to thank P. Pirotte and M. Cadet for their precious help that allows us to perform our research daily. Acknowledgments go also to W. Stone and J. Jeener for reading the manuscript. Finally, J.R. thanks H. Musso for allowing the completion of this paper from oversea. This work was supported by the BNB (Banque Nationale de Belgique).

*Present address: Institute of Nanoscale Science and Engineering, Vanderbilt University, Nashville, TN 37235, USA; Electronic address: John.Rozen@Vanderbilt.edu

¹J. D. Crane, P. B. Hitchcock, H. W. Kroto, and D. R. M. Walton, J. Chem. Soc., Chem. Commun. **1992**, 1764.

²P. Espeau, M. Barrio, D. O. López, J. L. Tamarit, R. Céolin, H.

Allouchi, V. Agafonov, F. Masin, and H. Szwarc, Chem. Mater. **14**, 321 (2002).

³A. Kubo, R. Ikeda, and D. Nakamura, J. Chem. Soc., Faraday Trans. 2 **82**, 1543 (1986).

⁴P. Seiler and J. D. Dunitz, Acta Crystallogr., Sect. B: Struct. Crystallogr. Cryst. Chem. **35**, 1068 (1979).

- ⁵R. K. Bohn and A. Haaland, *J. Organomet. Chem.* **5**, 470 (1966).
- ⁶A. Haaland and J. E. Nilsson, *Acta Chem. Scand.* (1947-1973) **22**, 2653 (1968).
- ⁷E. Shabanova, K. Schaumburg, and F. S. Kamounah, *Can. J. Anal. Sci. Spectrosc.* **43**, 53 (1998).
- ⁸J. Rozen, R. Céolin, J. L. Tamarit, H. Szwarc, and F. Masin, in *Molecular Nanostructures, XVII International Winterschool/Euroconference on Electronic Properties of Novel Materials*, edited by H. Kuzmany, J. Fink, M. Mehring, and S. Roth, AIP Conf. Proc. No. 685 (AIP, Melville, NY, 2003) pp. 19–22.
- ⁹A.-S. Grell, F. Masin, R. Céolin, M. F. Gardette, and H. Szwarc, *Phys. Rev. B* **62**, 3722 (2000).
- ¹⁰R. K. Boyd, C. A. Fyfe, and D. A. Wright, *J. Phys. Chem. Solids* **35**, 1355 (1974).
- ¹¹C. A. Fyfe and D. Harold-Smith, *J. Chem. Soc., Faraday Trans. 2* **71**, 967 (1975).
- ¹²C. A. Fyfe and D. Harold-Smith, *Can. J. Chem.* **54**, 769 (1976).
- ¹³A. J. Campbell, C. A. Fyfe, D. Harold-Smith, and K. R. Jeffrey, *Mol. Cryst. Liq. Cryst.* **36**, 1 (1976).
- ¹⁴D. E. Williams, *Science* **147**, 605 (1965).
- ¹⁵D. E. Williams, *J. Chem. Phys.* **45**, 3770 (1966).
- ¹⁶D. E. Williams, *J. Chem. Phys.* **47**, 4680 (1967).
- ¹⁷D. E. Williams, *Acta Crystallogr., Sect. A: Cryst. Phys., Diffr., Theor. Gen. Crystallogr.* **25**, 464 (1969).
- ¹⁸D. E. Williams, *Trans. Am. Crystallogr. Assoc.* **6**, 21 (1970).
- ¹⁹H. S. Johnston, *Gas Phase Reaction Rate Theory* (Ronald, New York, 1966).
- ²⁰M. R. Churchill and J. Wormald, *Inorg. Chem.* **8**, 716 (1969).
- ²¹N. Bloembergen, E. M. Purcell, and R. V. Pound, *Phys. Rev.* **73**, 679 (1948).
- ²²R. Kubo and K. Tomita, *J. Phys. Soc. Jpn.* **9**, 888 (1954).